TOWARDS CONTINUOUS RESISTANCE WELDING FOR FULL-SCALE AEROSPACE COMPONENTS

Manuel Endrass[1], Simon Thissen[1], Stefan Jarka[1], Marc-Andre Octeau[2], Marc Palardy-Sim[2], Julieta Barroeta Robles[2], Lars Larsen[1], Ali Yousefpour[2], and Michael Kupke[1]

[1] German Aerospace Center (DLR),
Center for Lightweight Production Technology, (ZLP), Augsburg, Germany

[2] National Research Council Canada (NRC),
Aerospace Manufacturing Technology Center, Aerospace Research Center,
Montreal, Quebec, Canada

ABSTRACT

This paper presents the preliminary stages of the collaboration between the National Research Council Canada (NRC) and the German Aerospace Center (DLR). A study demonstrating the current status of continuous resistance welding and the efforts to increase the process maturity is presented. Furthermore a continuous resistance welding end-effector concept developed at the DLR's Center for Lightweight Production Technology (ZLP) Augsburg is discussed in this work.

1. INTRODUCTION

Due to the high capital commitment in major component assembly as well as final assembly line in aircraft production, it is particularly worthwhile to improve workflow and reduce lead times here. The weldability of carbon fiber-reinforced thermoplastic composites is seen as one of the enablers to re-imagine assembly processes, reducing part count as well as reducing the overall assembly time. Resistance welding is one of the most promising technologies for assembling thermoplastic composites to full-scale aerospace structures because of its high achievable weld strength and potential for simple process monitoring and control. Static resistance welding is a relatively mature process; however, it lacks scalability, and quickly becomes non-feasible for metres-long aircraft structural joints. The continuous resistance welding process is a viable solution for long weld seams, such as longitudinal or circumferential seams on an aircraft fuselage. But the process maturity of continuous resistance welding is not yet at the same level compared to static resistance welding.

1.1 Resistance welding of high performance thermoplastics

Resistance welding uses Joule heating to locally melt the interface between two components. A welding element, consisting of an electrical conductor encased in an electrical insulator, is placed between two components. The electrical conductor remains in the bondline following the weld, thus care must be used to select a compatible material. Furthermore, neat resin film is often used as the insulating material in order to fill the gaps of the electrical conductor and to provide a resin rich area pre-melting for proper melt flow at the welding interface. A welding pressure is applied externally to the weld seam and an electrical voltage is applied to the welding element.

According to the Joule-Lenz law, the current-carrying conductor heats up. For semi-crystalline thermoplastics, the welding pressure must be maintained until reaching the post-crystallization temperature of the material. On the other hand, for amorphous thermoplastics, the pressure is kept until the temperature is below the glass transition temperature (T_g) of the material. Metallic fabrics as well as carbon fiber fabrics or unidirectional carbon fibers can be used as electrical conductor material [1], [2]. Figure 1 shows a schematic setup for static resistance welding.

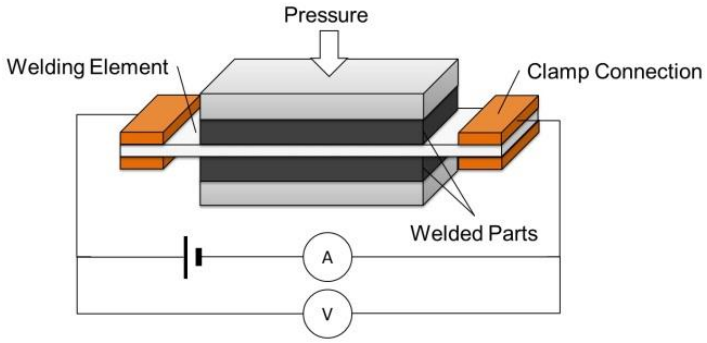

Figure 1 Schematic setup of static resistance welding (adapted from [3]).

1.2 Lack of scalability of static resistance welding

Mc. Knight et al defined a resistance weld to be "large scale when a specific level of thermal uniformity cannot be maintained in the bond areas for a range of welding power levels" [4]. The challenges faced when scaling the process of static resistance welding is maintaining temperature uniformity across the weld area, excessive power requirements, maintaining a homogeneous weld pressure, and challenges related to the physical layout of the parts to be welded (e.g. assembly and stacking sequence).

Temperature uniformity is an essential aspect in order to generate high weld strengths with low scatter. Increasing the weld length (parallel to the direction of current flow) results in an increase in voltage drop-off. The magnitude of the voltage becomes an issue particularly when welding electrically conductive components like carbon fiber reinforced thermoplastics (CFR-TP's), where current leakage can be observed through the carbon fibres. The likelihood of current leakage occurring is further increased at elevated welding temperatures as the higher temperature increases resin mobility, enabling movement of the electrically conductive components, resulting in the risk of new electrical pathways being formed. Thus, most of the resistance welds of electrical conductive components discussed in literature require additional matrix [5], glass fiber (GF) [6] or Titaniumdioxide (TiO_2) [7] isolation material between the electrically conductive element and the CFR-TP laminates.

Increasing the weld width (perpendicular to the direction of current flow), increases the current necessary to heat up the interface. Generally, resistance welding has relatively high power requirements to rapidly heat up the weld interface. For high performance thermoplastics, power densities have been shown on the order of 10s to 100s of kW/m^2 [8], [9]. Thus, as weld width increases, this power level quickly becomes unfeasible, and risks for non-uniformities and hot spots drastically increases.

A homogenous welding pressure is essential for generating high quality welds as a reduced pressure results in an increased void content along the weld interface [10]. In static resistance welding, generally, a welding pressure on the order of 1 MPa showed the best Single Lap Shear (SLS) strength results with acceptable squeeze flow around the edges [8]. Application of the required welding pressure over an entire aircraft fuselage longitudinal joint, for example, will lead to many challenges ensuring pressure homogeneity due to the geometric tolerance of the various fixture components. In this example, the continuous resistance welding process would be beneficial as it focuses the temperature, pressure, and power onto a particular welding spot.

2. CONTINUOUS RESISTANCE WELDING ON COUPON LEVEL

2.1 Continuous resistance welding process principle

In order to address the scalability challenges inherent to static resistance welding, continuous resistance welding was developed. In this process, a mobile end-effector travels along the width of the weld, applying power to the welding element and locally melting the polymer between the electrode contact points, while pressure is applied over the melt region to ensure complete weld consolidation. This is shown schematically in Figure 2, where a simple welded doubler coupon is depicted. In this figure, the end-effector travels along the x-axis while current flows in the perpendicular direction, along the y-axis.

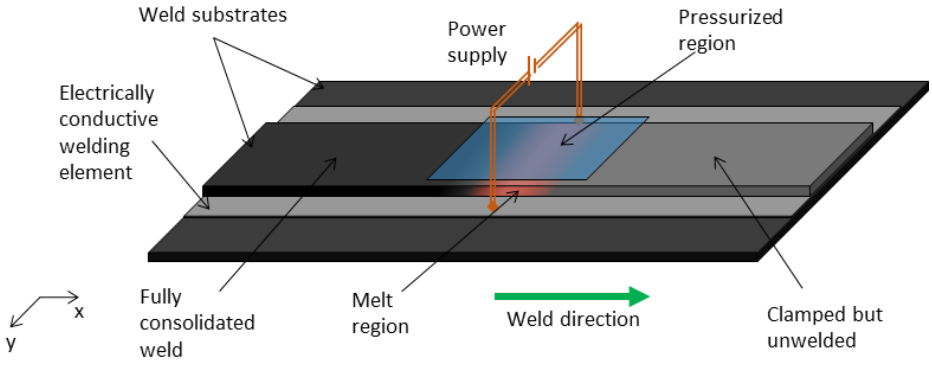

Figure 2 Continuous resistance welding schematic.

A modification to this method [11] discretizes the power input to a long weld seam using separated electrode block connectors; however, the conductive mesh is continuous. Thus, as the end-effector advances, current flows between the connectors, heating the laminate locally to produce the melt zone. Since it is a continuous process, a small amount of material ahead of and behind the melt zone is also heated. This enables a weld free of edge effects along its width (perpendicular to the direction of current flow) with a slower polymer cool-down, improving crystallization, when applicable. Pressure is applied locally, encompassing the entire melt zone, ensuring the weld is pressurized until the interface temperature drops below the necessary polymer transition temperature. The total pressure requirements are limited through the use of a compaction roller or shoe.

There are a number of process parameters (e.g.: end-effector speed, applied voltage level, welding pressure, etc.) as well as setup parameters (e.g.: electrode contact size, compaction length, etc.) that must be precisely tuned for each material type and weld length.

Recall that weld length is defined as the distance between electrode contact points, parallel to the direction of current flow. Since it is a continuous process, once a process is optimized, it can be applied to any joint length required. Resistance welding is a low-flow composite joining technique, and many of the fundamental phenomena are well understood and described analytically. Thus, process modelling has been demonstrated as an effective approach for accurately selecting and optimizing process parameters.

2.2 Test bench description

A test bench setup was developed by the NRC to demonstrate the continuous resistance welding process and is shown in Figure 3 (top and bottom views). The setup consists of a vertically translating end-effector to apply compaction pressure to the weld zone and a horizontally translating stage to align and translate the weld coupon. Pneumatic pistons (1 in Figure 3) control the bulk displacement of the end-effector and apply the vertical welding pressure. Pressure is applied via a series of small compaction rollers (3) and a semi-rigid pressure distribution plate (2) is placed on top of the weld interface, providing thermal insulation and insuring a smooth pressure distribution.

A smaller set of pneumatic pistons (4) are used to raise and lower slip ring rotating copper electrodes (5), and to apply the appropriate clamping pressure to the weld element. This configuration is used to weld single lap shear test coupons, thus the slip ring electrodes are located on opposite sides of the weld interface, one connected to the end-effector head and the other connected to the base plate. Discrete copper blocks (6) are placed on top of the weld element, providing a smooth surface upon which electric power is applied. This produces a more uniform power distribution and prevents damage to the weld element due to the rotating slip ring electrode. Other elements in Figure 3 include the laminates (7), linear translation stage (8), and the electrical/thermal insulation and supporting fixture (9).

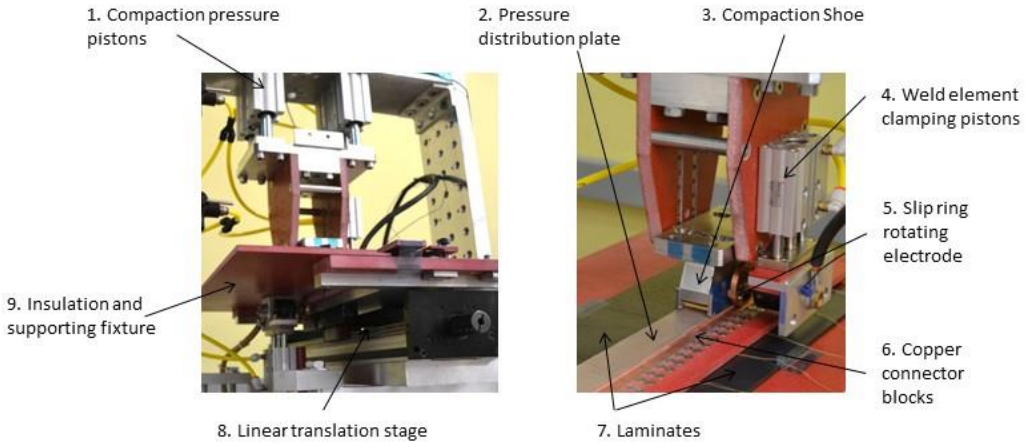

Figure 3 Single lap shear continuous resistance welding test bench setup.

This test bench was used to validate the continuous resistance welding process using many test cases over a range of high performance CFR-TPs. The data was used to validate a variety of thermal models used to predict weld temperature. For example, Shi et al. [12], developed a robust electrical and heat transfer process model to predict temperature distribution during the resistance welding of glass fiber reinforced PPS laminates. Numerous validation steps were

performed to verify many model parameters and assumptions. Ultimately, the predicted weld temperatures were shown to closely match the measured values (see Figure 4 a).
In another example, Zammar et al., developed another multi-physics based model for a different weld configuration [13], [14]. The model was shown to accurately predict interface temperature over a range of input voltages and end-effector speeds. The authors showed that using the model to predict surface temperature in a closed loop control system can accurately and repeatedly control interface temperature, producing a uniform temperature distribution during the welding operation compared to other approaches (see Figure 4 b).

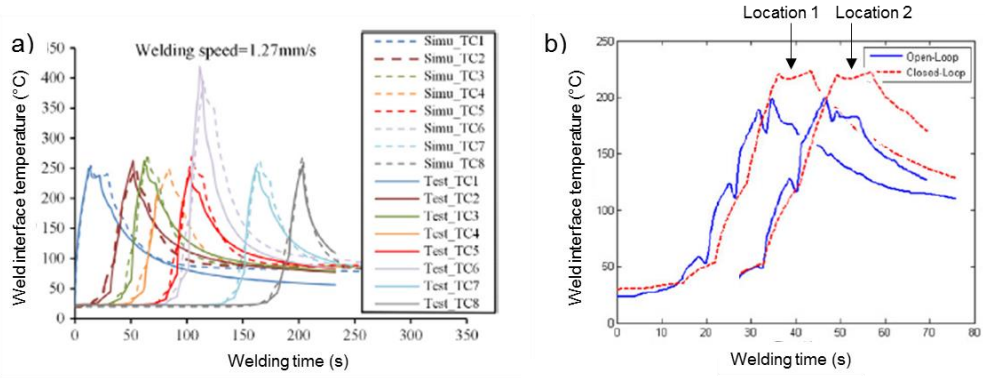

Figure 4 Thermal models developed by a) Shi et al. [12], and b) Zammar et al. [14] The experimental data was generated using the NRC test bench.

3. UPSCALING APPROACH

Due to the lack of scalability of static resistance welding and the requirement to perfom metres-long structural welds, the continuous resistance welding test bench developed by the NRC was redesigned by the DLR ZLP in Augsburg. A robotic end-effector was designed to address the challenges of this application beyond the test bench.

3.1 Investigation of different welding elements

In a first test series, an investigation of the heating behavior of different electrical conductors was performed. Here a carbon-fiber polyphenylenesulfide (CF/PPS) fabric, Toray CETEX® TC1100 (T300 3K, 5HS, 280GSM FAW, 43% RC), and a unidirectional carbon-fiber tape, Toray CETEX® TC1100 (Carbon AS4A 12K UD, 221 gsm FAW, 34% RC) [15], were used as electrical conductors. Steady state thermal images below the crystallite melting temperature, T_m, were captured using an Infratec VarioCAM® HD thermography camera.

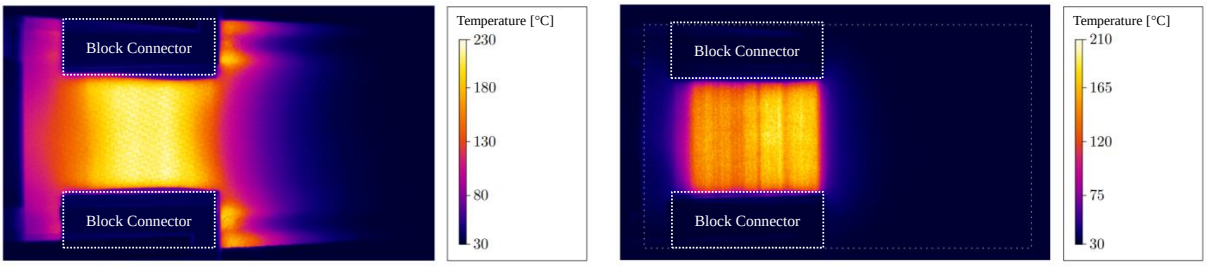

Figure 5 Steady state thermal images of a CF/PPS fabric (left) and CF/PPS unidirectional electrical conductor (adapted from [16]).

The thermal images shown in Figure 5 highlight the differences in heating behavior of the CF/PPS fabric and unidirectional electrical conductor. The CF fabric heats up a wider area across the electrode block connectors due to heat conduction and current flow along the transverse fibers next to the block connectors. The UD CF/PPS heating is concentrated between the electrode block connectors. These images can be correlated to current flow simulations performed by Shi [17] and Thissen [16]. For continuous resistance welding using a quasi-infinite carbon-fiber electrical conductor, a concentration of the heat in the weld seam is advantageous in order to avoid the generation of local hot spots in the unsupported section of the electrical conductor next to the electrode block connectors. Since the negative temperature coefficient (NTC) of the carbon fiber conductor favors the formation of local hotspots, further investigations were based on the unidirectional carbon fiber conductor.

3.2 Definition of contact- and consolidation principle

For the definition of a proper electrical contact strategy, two different variants for current introduction in the form of a line contact (wheel) and a surface contact (block connector) were investigated by thermography. Both variants showed an adequate heating behavior of the unidirectional carbon-fiber conductor on the coupon level (Figure 6).

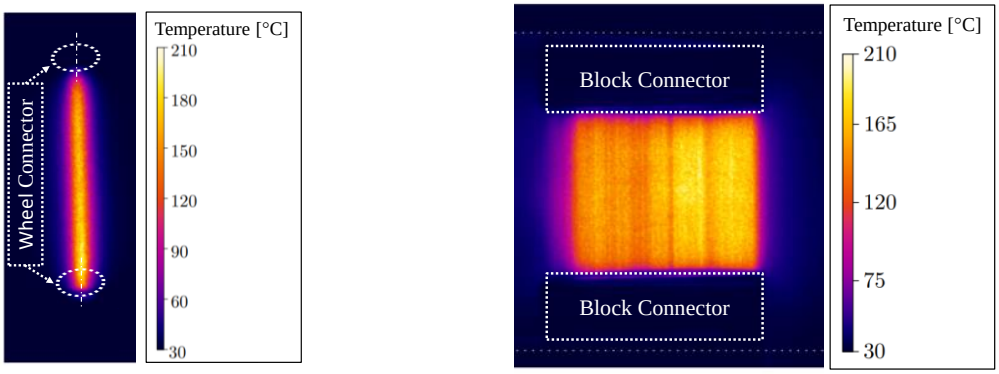

Figure 6 Comparison of a wheel connector (left) and a block connector (right) for current introduction into a UD CF/PPS ply

Due to the electrode contact pressure-resistance dependency, it is critical to ensure a uniform electrode contact pressure. For simple, flat structures, an elongated electrode block connector would distribute power over a larger area uniformly, as shown above. However, in general, for applications outside the optimal test environment, the geometrical coincidence between the electrode block connector and the welding conductor cannot be guaranteed and a wheel connector may be required. Thus, selection of the appropriate electrode format will vary based on the application to ensure a uniform contact pressure and homogeneous heating.

It must be ensured that an even welding pressure is applied beyond the heated area of the joint to achieve a void-free interface without deconsolidation at the boundaries. Two basic principles were validated in a preliminary test series for the application of the welding pressure, an inflatable membrane and a high temperature elastomer belt (Wacker ELASTOSIL® M 4470). For validation of the pressure uniformity, Fujifilm Prescale pressure measuring film was used.

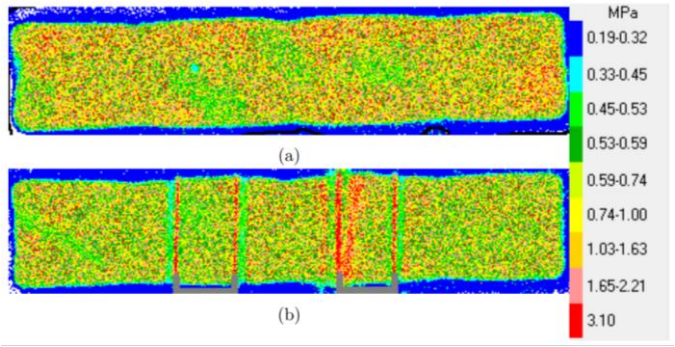

Figure 7 Pressure distribution of the inflatable membrane at 0.6MPa welding pressure without (a) and with (b) steps in the organosheet

Figure 7 shows the typical welding pressure distribution for the inflatable membrane, where small steps in the laminate stacking sequence show a minor impact on the consolidation uniformity. These are highlighted by narrow lines with increased pressure in Figure 7 b). The elastomeric belt showed a slightly reduced uniformity of welding pressure; however, it could be more easily integrated into an end-effector. Furthermore, with the elastomeric belt, pressure is distributed uniformly over the entire weld seam length (distance between electrodes, parallel to the current flow) up to the electrical contacts and simplifies the end-effector design. Thus it was the chosen concept for the application of welding pressure.

3.3 End-effector design

The end-effector for continuous resistance welding has a modular design and was designed and manufactured at the DLR ZLP in Augsburg. The end-effector is shown in Figure 8. The wheel connector module can be interchanged with a block connector in order to perform further investigations regarding the electrode contact principle. The image on the right hand side shows both wheel connectors (1) which introduce the welding current and the elastomer belt (2) which serves for the uniform application of the welding pressure. The figure shows an example setup connecting two CFR-TP components (5) using a butt strap (3), with access on one side of the welding element (4). Possible application scenarios were defined as the production of a single lap weld as well as a simple lashing. These joint variants are often used for aircraft longitudinal and circumferential seams.

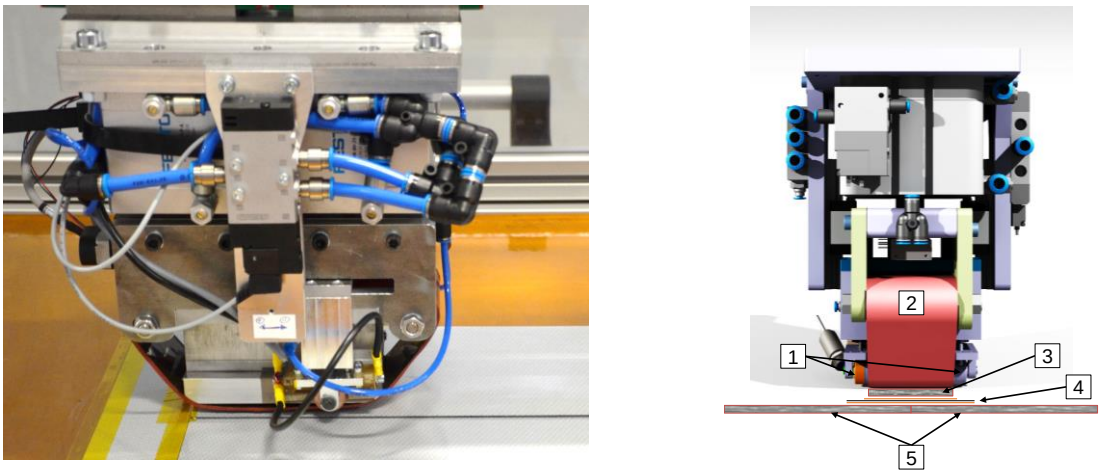

Figure 8 End-effector for continuous resistance welding in side view (left) and front view (right) [16]

3.4 First investigations

The end-effector technology was tested and the process validated on a simple linear axis without a robot. First, tests were carried out to verify the functionality of the end-effector. Static welding and preliminary continuous resistance welding measurements were performed. The static welding process showed no abnormalities and ran smoothly, as expected. The resistance value between the two copper wheels was measured at a constant end-effector velocity along the traverse path of 0.3 mm/s (Figure 8).

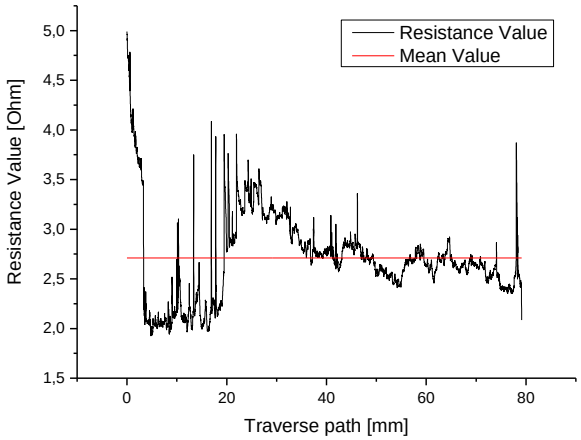

Figure 9 Resistance value along the traverse path at a constant end-effector velocity of 0.3mm/s

The resistance value of the electrical conductor has a direct influence on the temperature development of the weld interface. Fluctuations in resistance means a varying amount of current will pass through the electrical conductor for a given voltage level. A standard deviation of the resistance value of 17% compared to the average value, as observed in the first investigations, was deemed insufficient and requires further investigation.

4. SUMMARY

This paper presents excerpts from the preliminary work on continuous resistance welding carried out by the NRC and the work based on it by DLR ZLP Augsburg. The principle of static and continuous resistance welding, different electrical conductors and isolation methods were described. Furthermore the lack of scalability of the static resistance welding process was discussed with emphasis on power level limitations, the maintenance of a homogeneous welding pressure, the physical layout of the parts to be welded and the process temperature uniformity. A test bench for continuous resistance welding on the coupon level and the process principle behind it were described. Here the electrical current was introduced by a number of block connectors on opposite sides of the weld seam and the melt zone is continuously shifted perpendicular to the current flow along the weld seam. Investigations into the heating behavior of different carbon-fiber welding elements were performed showing a focused heating of the unidirectional CF/PPS electrical conductor. Measurements on welding pressure with two different elastomeric materials were conducted demonstrating a homogenous pressure distribution over the weld seam. Finally an end-effector with focus on robotic continuous resistance welding was designed and the first investigations were presented.

5. REFERENCES

[1] D. Stavrov und H. Bersee, „Resistance welding of thermoplastic composites - an overview," *Composites Part A: Applied Science and Manufacturing,* Nr. 36, pp. 39-54, 2005.

[2] A. Yousefpour, M. Hojjati und J.-P. Immarigeon, „Fusion Bonding/Welding of Thermoplastic Composites," *Journal of Thermoplastic Composite Materials,* Nr. 17, pp. 303-341, 2004.

[3] D. Stavrov und H. E. N. Bersee, „Thermal Aspects in Resistance Welding of Thermoplastic Composites," in *ASME 2003 Heat Transfer Summer Conference,* 2003.

[4] S. H. Mc Knight, S. T. Holmes, J. W. J. Gillespie, C. L. T. Lambing und J. M. Marinelli, „Scaling Issues in Resistance-Welded Thermoplastic Composite Joints," in *Advances in Polymer Technology, Vol. 16, No. 4,* John Wiley & Sons, Inc., 1997, pp. 279-295.

[5] E. C. Eveno und J. W. J. Gillespie, „Resistance Welding of Graphite Polyetheretherketone Composites: An Experimental Investigation," *Journal of THERMOPLASTIC COMPOSITE MATERIALS, Vol. 1,* pp. 322-338, October 1988.

[6] C. Freist, Experimentelle und numerische Untersuchungen zum Widerstandsschweißen endlosfaser- und kurzfaserverstärkter thermoplastischer Hochleistungsstrukturen, Stuttgart: Institut für Flugzeugbau (IFB) der Universität Stuttgart, 2013.

[7] M. Dubé, P. Hubert, A. Yousefpour und J. Denault, „Current leakage prevention in resistance welding of carbon fibre reinforced thermoplastics," *Science Direct, Composites Science and Technology,* p. 1579–1587, 2008.

[8] C. Ageorges, L. Ye und M. Hou, „Experimental investigation of the resistance welding of thermoplastic-matrix composites," *Composites Science and Technology,* Nr. 60, pp. 1027-1039, 2000.

[9] M. Dubé, P. Hubert, A. Yousefpour und J. Denault, „Resistance welding of thermoplastic composites skin/stringer joints," *Composites Part A: Applied Science and Manufacturing,* Nr. 38, pp. 2541-2552, 2007.

[10] H. Shi, I. Fernandez Villegas und H. E. Bersee, „A STUDY OF PROCESS INDUCED VOIDS IN RESISTANCE WELDING OF THERMOPLASTIC COMPOSITES," in *20th International Conference on Composite Materials,* Copenhagen, 2015.

[11] A. Yousefpour und M.-A. Octeau, Resistance Welding of Thermoplastics, U.S. Patent 11/887 847, 2005.

[12] H. Shi, I. Fernandez Villegas, M.-A. Octeau, H. E. Bersee und A. Yousefpour, „Continuous resistance welding of thermoplastic composites: Modelling of heat generation and heat transfer," *Composites Part A: Applied Science and Manufacturing,* Nr. 70, pp. 16-26, 2015.

[13] I. A. Zammar, I. Mantegh, M. S. Huq, A. Yousefpour und M. Ahmadi, „A three-dimensional transient model for heat transfer in thermoplastic composites during continuous resistance welding," *Advanced Manufacturing: Polymer & Composites Science,* pp. 32-41, 26 April 2017.

[14] I. A. Zammar, I. Mantegh, M. Saiful Huq, A. Yousefpour and M. Ahmadi, "Intelligent Thermal Control of Resistance Welding of Fiberglass Laminates for Automated

Manufacturing," *IEEE/ASME Transactions on Mechatronics,* vol. 3, no. 20, pp. 1069-1078, June 2015.

[15] T. A. Composites, „Cetex TC1100_PDS_v5_2019-11,“ [Online]. Available: https://www.toraytac.com/media/221a4fcf-6a4d-49f3-837f-9d85c3c34f74/itF97A/TAC/Documents/Data_sheets/Thermoplastic/UD%20tapes,%20prepregs%20and%20laminates/Toray-Cetex-TC1100_PPS_PDS.pdf. [Zugriff am 27 April 2020].

[16] S. Thissen, *Entwicklung, Aufbau und Validierung eines Endeffektors zum kontinuierlichen Widerstandsschweißen faserverstärkter Hochleistungsthermoplaste,* Zentrum für Leichtbauproduktionstechnologie (ZLP) Augsburg, Institut für Flugzeugbau (IFB) der Universität Stuttgart, 2020, p. 96.

[17] H. Shi, Resistance weldingofthermoplastic composites, Delft: Technical University Delft, 2014.

[18] H. Shi, Resistance welding of thermoplastic composites, Delft: Technical University Delft, 2014.

[19] A. Yousefpour und M.-A. Octeau, „Resistance Welding of Thermoplastics“. EP WO US CA Patent US20090032184A1, 2005.